Food Structure 37 (2023) 100332

Contents lists available at ScienceDirect

Food Structure

journal homepage: www.elsevier.com/locate/foostr

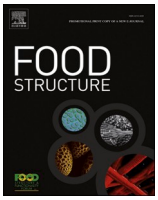

Gelling capacity of cell-disrupted *Chlorella vulgaris* and its texture effect in extruded meat substitutes

Cora De Gol [a,b], Silvia Snel [a,c], Ysamar Rodriguez [a], Michael Beyrer [a,*]

[a] University of Applied Sciences and Arts Western Switzerland, School of Engineering, Sion, Switzerland
[b] Food Microbiology, Wageningen University & Research, Wageningen, the Netherlands
[c] Food Process Engineering, Wageningen University & Research, Wageningen, the Netherlands

ARTICLE INFO

Keywords:
Microalgae
Pea protein isolate
High-pressure homogenization
Gelation properties
High-moisture extrusion cooking
Plant-based foods

ABSTRACT

Microalgae attract increasing interest in enhancing the nutritional values of plant-based foods. However, alterations in the final product's color (by green algae) and mushy texture can be induced. In this study, we incorporated yellow *Chlorella vulgaris* (Cv) in pea protein-based meat substitutes and aimed to minimize properties alteration by using wet and disrupted Cv biomass. The cell wall disruption, done by high-pressure homogenization (HPH) at 150 MPa and initial biomass temperature below 10 °C, significantly increased the gelation capacity. The effect was confirmed by (i) a 10x increase in the apparent viscosity of 14% (w/w) Cv suspensions, and (ii) a 2x increase in the storage modulus (G') of 9:1 (w/w) pea protein isolate - Cv gels. Furthermore, the HPH-treated Cv was successfully incorporated (10% (w/w)) into pea protein-based meat substitutes produced with high-moisture extrusion cooking without altering their visual appearance, hardness, or anisotropy index. Finally, spray drying or fractionation steps of the HPH-treated Cv did not improve protein gels, or meat substitutes produced thereof. This study demonstrated that disrupted Cv is a promising nutritious and sustainable ingredient for meat substitutes.

1. Introduction

Plant-based diets are gaining importance thanks to their lower environmental footprint and positive effect on overall consumer health. However, such diets increase the risks of deficiencies in certain nutrients such as vitamin B12, choline, and calcium (Chen et al., 2019). As a solution, microalgae emerge as promising candidates for fortifying plant-based foods (Caporgno & Mathys, 2018). They contain all essential amino acids, vitamin B12, calcium, soluble fibers, and essential fatty acids (Barka & Blecker, 2016; Becker, 2007; Bito et al., 2020; Demarco et al., 2022; Grossmann et al., 2020). Moreover, microalgae have a low land requirement, high protein content, and a fast growth rate. Therefore, they are considered as promising raw material to produce sustainable food (Kusmayadi et al., 2021; Smetana et al., 2017).

Examples of microalgae that are currently used in food products are *Arthospira spp.* and *Chlorella spp.* (Lafarga, 2019). Interestingly, phototrophic, heterotrophic and mixotrophic cultivations of *Chlorella vulgaris* (Cv) are possible. The growth conditions, i.e., the light intensity and the agitation rate, influence the microorganism's protein content (Canelli et al., 2020a; Imamoglu, 2015; Seyfabadi et al., 2011). Typically, Cv contains 51 – 58% crude proteins, 14 – 22% lipids, and 12 – 17% carbohydrates on dry basis (Oppen et al., 2022). Of the proteins, 50% are inside the cell, 20% are bound to the cell wall, and 30% can migrate in and out of the cell (Safi et al., 2014). Cv has rigid cell walls composed of chitosan, cellulose, hemicellulose, proteins, lipids, and minerals (Safi et al., 2014). Thus, to extract the intercellular proteins, the cell walls must be disrupted. Several authors demonstrated that mechanical cell wall disruption like high-pressure homogenization (HPH) and bead milling results in the release of intracellular proteins, as well as an increase in protein digestibility, and bioavailability of vitamins and minerals, which were confirmed by *in vitro* assays (Bito et al., 2020; Canelli et al., 2020b; Demarco et al., 2022; Wang et al., 2020). Additionally, cell wall disruption modifies microalgae biomass functionality such as gelation capacity (Bernaerts et al., 2017). HPH has been proven to be the most effective technique (Grossmann et al., 2020), not only for achieving complete cell disruption (for Cv at 150 MPa, 3 passes) (Carullo et al., 2018) but also for being energy efficient (Safi et al., 2017). Following cell disruption, centrifugation can separate soluble from insoluble fractions (Grossmann et al., 2020). In general, the microalgae ingredient is dried to facilitate its storage and extend its shelf life.

* Correspondence to: Rue de l'Industrie 19, 1950 Sion, Switzerland.
E-mail address: michael.beyrer@hevs.ch (M. Beyrer).

https://doi.org/10.1016/j.foostr.2023.100332
Received 27 March 2023; Received in revised form 3 June 2023; Accepted 6 June 2023
Available online 9 June 2023

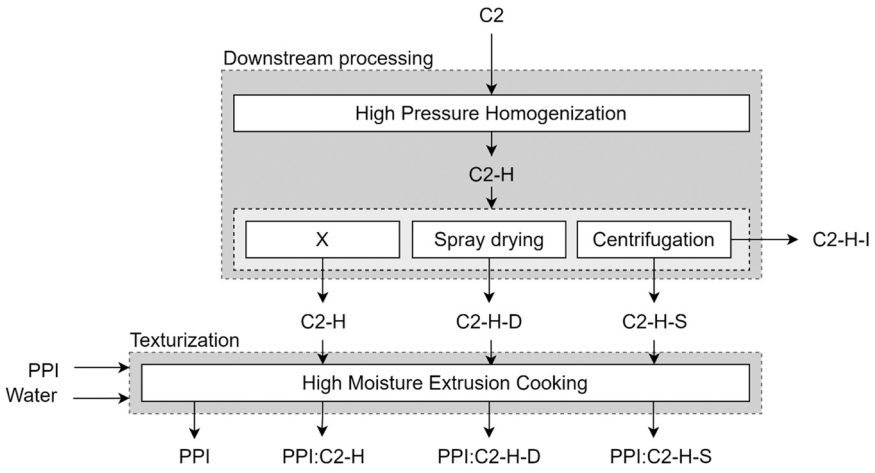

Fig. 1. Schematic overview of the DSP of microalgae and application in HMEC. C: *Chlorella*, H: homogenized, X: no additional DSP, D: spray-dried, S: soluble fraction, I: insoluble fraction, PPI: pea protein isolate.

However, drying showed some limitations such as product quality degradation and digestibility reduction, as well as high energy and cost requirements (Show et al., 2015). Cell disruption, centrifugation and drying are referred as downstream processing (DSP) steps.

The addition of microalgae to meat substitutes was identified as a promising route to improve their nutritional profile (Fu et al., 2021). Meat substitutes can be produced with high-moisture extrusion cooking (HMEC), among other techniques (Dekkers et al., 2018). Typically, HMEC involves the hydration and mixing of high protein powder ingredients with water (50–70% moisture), cooking under high shear, pressure, temperature, and cooling through a long die where elongated proteins align into a fibrous texture (Cornet et al., 2022). Ingredients that can be produced into fibrous meat substitutes include pea and soy protein isolates and concentrates, often in combination with starch, fibers, and gluten, due to their high functionality and texturizing capacity (Cornet et al., 2022; Yao et al., 2004). So far, the addition of *Arthrospira platensis* has been tested in soy and lupin meat substitutes produced with HMEC (Grahl et al., 2018; Palanisamy et al., 2019). However, the addition of *Arthospira platensis* results in dark green-colored meat substitutes. The use of microalgae after chlorophyll removal was thus suggested to obtain a more acceptable color (Fu et al., 2021). Under the right cultivation conditions, *Chlorella spp.* can accumulate carotenoid pigments instead of chlorophylls, resulting in yellow biomass (Caporgno et al., 2019).

The focus of this study is to improve the heat-induced gelation properties of the Cv biomass by homogenization and incorporate the homogenized biomass without drying, into pea protein-based extruded meat substitutes. The goal is to obtain extrudates with unaltered texture, but enriched with microalgae. To the best of the authors' knowledge, no studies have examined the incorporation of wet, yellow, and disrupted Cv biomass as an ingredient in HMEC.

2. Materials and methods

2.1. Materials

Two freshly produced Cv biomasses (C1 and C2) were kindly donated by Alver AG (Switzerland). Microalgae were heterotrophically cultivated in two different batches by Phycom (The Netherlands) using a patent-protected yellow *Chlorella vulgaris UTEX 30* strain (Uran et al., 2021). Directly after harvesting, the biomasses were centrifuged, and the concentrated biomasses were packed in 5 kg bags, frozen and sent in insulation boxes. The frozen biomasses were stored at − 20 °C until use and transferred to a cooling chamber (4 °C) the day before the trial for defrosting. Their dry matter (DM) was 25.0 ± 0.2% and 26.0 ± 0.3% (w/w), respectively. The defrosted biomasses were diluted with deionized water to 13.2 ± 0.0% and 13.8 ± 0.0% (w/w) DM. Their respective pH values were 6.4 ± 0.1 and 5.4 ± 0.0. Moisture content analysis was done using the rapid moisture analyzer (HC103 Mettler-Toledo) at the conditions of 120 °C, initial mass of 2 g, and stop criteria of 1 mg/50 s. The pH of the suspensions was measured with a pH meter 914 (Metrohm, Switzerland). C1 was used to optimize the HPH treatment, whereas C2 was intended for HMEC trials. The amino acid profile of C1 was analyzed by Eurofins Scientific (France) (Table A2) and was used to calculate the nitrogen-to-protein conversion factor (f) (Eq. (1)). Using Eqs. (2) and (3), a value of 4.21 was obtained.

$$f = 1 \Big/ [N]_{prot} \tag{1}$$

$$[N]_{prot} = \sum_{i=1}^{18} [N]_{AA,i}\left(g_N / g_{prot}\right) = \sum_{i=1}^{18} [AA]_{prot,i}\left(g_{AA} / g_{prot}\right) \cdot [N]_{AA,i}\left(g_N / g_{AA}\right) \tag{2}$$

$$[N]_{AA,i}\left(g_N / g_{AA}\right) = n_N \Big/ \left(Mw_{AA,i} - Mw_{H_2O}\right)\left(mol / g_{AA}\right) \cdot Mw_N\left(g_N / mol\right) \tag{3}$$

With n_N the number of nitrogen atoms per amino acid, $[N]_{prot}$ and $[N]_{AA,i}$ the mass concentration of nitrogen in proteins and amino acids, respectively. *Mw* is the molecular weight.

Commercial pea protein isolate (PPI) (Nutralys® F85M) was obtained by Roquette Frères S.A. (Lestrem, France). The minimum protein content (f = 6.25) on DM was given by the supplier and was 83% (w/w). The moisture content was 7.5% (w/w).

2.2. Cell disruption by HPH

Cv cell disruption was done by HPH using a NS3006L ARIETE homogenizer (GEA Niro Soavi, Italy) equipped with a radial diffuser homogenization valve. Different operating pressures and initial product temperatures were studied. C1 was used to find the HPH optimal conditions.

First, the effect of pressure (90, 120 or 150 MPa, 1 pass) at initial temperature of 5 ± 1 °C was tested. Product flow rates were 64, 54 and 48 L/h for each pressure, respectively. A heat exchanger (cold tap water, 12 °C) was installed immediately after the homogenization valve to quickly cool down the product after HPH treatment. HPH-treated Cv suspensions were labeled as C1-H-90, C1-H-120 and C1-H-150. For each pressure, a second pass was also tested. The product was cooled down between the passes using an ice bath to reach a temperature of 5 ± 2 °C.

Second, the effect of initial temperature (T_{in}) (5, 10, 15, 20 and 25 °C) at a fixed operating pressure (Δp) of 150 MPa and 1 pass was

tested. The process temperature (T_p) (°C) during HPH treatment was estimated using Eq. (4) (Osorio-Arias et al., 2020):

$$T_p = T_{in} + \delta \cdot \Delta p + \xi \cdot \Delta p - \sum heat \quad loss \tag{4}$$

The terms δ and ξ correspond to the temperature change due to the heat of compression and homogenization, respectively, and were approximated to 8 °C/100 MPa and 18 °C/100 MPa for a worst-case scenario. Heat losses were considered negligible (Osorio-Arias et al., 2020).

Third, cell disruption of C2 was done at the identified HPH optimal pressure and initial temperature conditions (150 MPa, 5 – 10 °C, 1 pass). The treated suspension was named C2-H. The protein, lipid, and carbohydrate contents of C1-H-150 and C2-H were analyzed externally by the Swiss Quality Testing Services (SQTS) (Switzerland).

2.3. Downstream processing (DSP) of microalgae biomass

To study the effect of DSP steps, namely centrifugation and spray-drying, on the gelation capacity of the HPH-treated Cv suspensions, C2-H was split in three parts. One part was centrifuged, another was spray-dried, and one was kept intact and used as a reference. All three preparations were used for rheological characterization, gel formation with PPI, and partial replacement of PPI in the production of extrudates by HMEC (Fig. 1).

2.3.1. Centrifugation

Centrifugation was done at 8000 *g* at 4 °C for 10 min, using a lab-scale centrifuge Sigma 3–16KL (Adulf Kühner AG, Switzerland). The supernatant or soluble fraction (C2-H-S) was kept at 4 °C in closed containers until use. The insoluble fraction (C2-H-I) was discarded.

2.3.2. Spray drying

Spray drying was done using a mobile minor MM-PSR spray dryer (GEA Niro Soavi, Italy). The operating set conditions were 0.1 MPa pressure, 103 kg/h flow rate of drying air, 180 and 103 °C inlet and outlet air temperatures, respectively. The product was pumped using a peristaltic pump NEMA 4X IP66 (Watson Marlow, United Kingdom) at 9 rpm, corresponding to a product flow of 2 kg/h.

2.4. Characterization of microalgae preparations

2.4.1. Protein content and fraction of soluble protein

The protein content in dry basis was calculated from the total nitrogen (TN) (mg/L) value obtained using a total organic carbon/total nitrogen (TOC/TN) analyzer (Shimadzu, Japan) (Eq. (5). The auto dilution and injection volume were set at 2 and 100 μL, respectively. The dry weight (dw) is the DM of the sample before dilution expressed in mg/L. The f used was 4.21 (Section 2.1).

$$Protein \quad content \quad (\%) = f \cdot TN / \quad dw \cdot 100 \tag{5}$$

The fraction of soluble protein (Eq. (6)) was expressed as the amount of protein present in the supernatant (Eq. (5)) with respect to the initial amount of protein in the suspensions before centrifugation (from SQTS analysis). Centrifugation was done at 8000 *g* at 4 °C for 10 min on 5% (w/w) biomass and the supernatant was manually diluted 50x with deionized water before the TOC/TN measurement.

$$Fraction \quad of \quad soluble \quad protein \quad (\%) = prot_{supernatant} / prot_{suspension} \cdot 100 \tag{6}$$

2.4.2. Imaging

An optical microscope (Zeiss Axioplan, Germany) was used to observe the cell disruption level after HPH at different operating pressures. The samples were diluted 100x. The images were taken at a magnification of 40x and with a differential interference contrast (DIC0.5–1.4) filter.

2.4.3. Differential scanning calorimetry (DSC)

Heat-induced protein denaturation was determined by DSC using a μDSC7 evo (Setaram Instrumentation, France). A standard Hastelloy cylinder was filled with 600 μL of the sample (14% (w/w) DM). The reference cell was loaded with 600 μL of deionized water. The system was purged with a constant nitrogen flow at around 0.1 MPa. The samples were scanned from 20 °C to 100 °C at a heating rate of 0.5 °C/min, held at 100 °C for 10 min, and subsequently cooled to 20 °C at the same rate. The peak maximum temperature T_{peak} and the reaction enthalpy ΔH (J/g suspension) were obtained from the baseline integration of the endothermic peaks observed in the thermograms using the Thermal Analysis® Software package V. 1.46 (Setaram Instrumentation). The peak area was divided by the DM content of the suspension to obtain the ΔH in J/g DM.

2.4.4. Enzymatic hydrolysis

An enzymatic treatment was applied on C2-H to better understand the role of polysaccharides in the gelation mechanism. To target cellulose and hemicellulose hydrolysis, two enzymes were used: a cellulase complex NS-22086 (Novozymes, Denmark) and an endo-xylanase NS-22083 (Novozymes, Denmark). The enzymatic treatment was done at 45 °C, for 2 h, at 120 rpm stirring speed, using 5.00% and 0.25% (w/w) cellulase and endo-xylanase, respectively. The pH of the biomass was not modified. The enzymatically hydrolyzed materials were studied by temperature sweep.

2.4.5. Temperature sweep (T-sweep)

The determination of the gelation capacity was done using the protocol described by Rodriguez & Beyrer (2023) with minor modifications. Briefly, the apparent viscosity (μ_{app}) as a function of temperature and time was obtained using a modular compact rheometer (MCR) model 302 (Anton Paar, Austria) equipped with an electrically heated temperature device, a counter-cooling concentric cylindrical system of 26 mm (C-ETD 160/ST) and a three-blade stirrer (ST24) measuring system. The Cv preparations were directly used at a DM of 14% (w/w) or diluted/rehydrated to 10.5% (w/w) with deionized water for better comparison with C2-H-S (due to DM reduction during centrifugation). The preparations were heated from 20 °C to 95 °C, held at this temperature for 5 min, and subsequently cooled to 20 °C. The heating and cooling rates were set at 6 °C/min and the stirring speed at 160 rpm. Data were obtained from the RheoCompass® software and firmware (Anton Paar, Austria) and treated to determine the initial viscosity ($\mu_{app,\ initial}$), final viscosity ($\mu_{app,\ final}$), and onset temperature (T_{onset}). Additionally, the peak viscosity ($\mu_{app,\ peak}$) during the heating interval was also determined and used to compare the gelation capacity between the different preparations.

2.4.6. Gel preparation

PPI-Cv gels were prepared by thermal-mechanical treatment (Tanger et al., 2020) following the method used by Rodriguez & Beyrer (2023) with minor modifications. The minimal gelling concentration of pea protein was reported to be close to 12% (Batista et al., 2011), therefore aqueous dispersions of higher DM were prepared. 17% DM (w/w) dispersions of 90% (w/w) PPI and 10% (w/w) Cv preparation (C2, C2-H, C2-H-S or C2-H-D) were stirred at 400 rpm for 5 min to ensure homogeneity. 100% PPI was taken as a reference. The dispersions were heated to obtain PPI-Cv gels using a MCR 302 (Anton Paar, Austria) equipped with a pressure cell (C-ETD 160/ST) and a three-blade stirrer (ST24-Pr) measuring system. Compressed air at 0.2 MPa was used to prevent burning above 100 °C. The dispersions were first mixed at 400 rpm for 30 s, followed by a stabilization interval at 160 rpm for 60 s. The dispersions were subsequently heated from 20 °C to 120 °C at 7.9 °C/min, held at this temperature for 300 s, and then cooled down to 20 °C at 7.9 °C/min. All three steps were performed with a rotational speed of 160 rpm. The formed gels were stored at 4 °C for 24 h before their characterization.

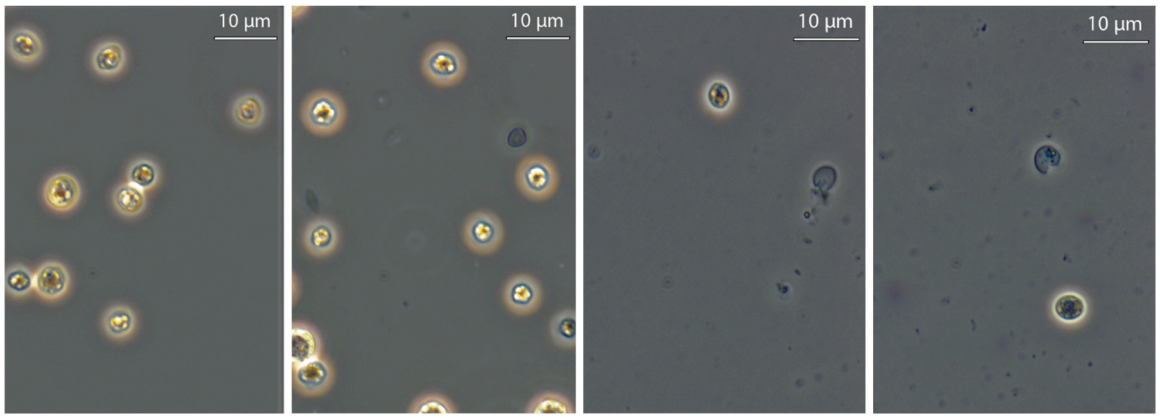

Fig. 2. Microscopic images of untreated (C1) and microalgae suspensions treated at 90, 120 and 150 MPa (14% DM, 5 °C, 1 pass) after dilution 100x and magnification 40x. From left to right: C1, C1-H-90, C1-H-120 and C1-H-150. Scale = 10 µm.

2.4.7. Amplitude sweep

Amplitude sweeps were performed to characterize the obtained gel preparations. A modular compact rheometer (MCR) model 302 (Anton Paar, Austria) fitted with Peltier temperature devise (P-PTD200/56), plate-plate geometry and PP25 measuring system was used. Samples were placed onto the lower plate and compressed between the plates up to a gap of 1 mm. Strain amplitude sweeps were performed at increasing deformation from 0.01% to 100% (logarithmic ramp), with a constant angular frequency of 3 rad/s and constant temperature of 20 °C. RheoCompass® software and firmware (Anton Paar, Austria) provided the storage modulus (G') (Pa), loss modulus (G'') (Pa), and shear stress (τ) (Pa) values for further analysis. For determining the linear viscoelastic (LVE) region, a limit of 3% of deviation of G' was used.

2.4.8. Confocal laser scanning microscopy (CLSM)

CLSM was used to visualize the microstructure of fresh gels. The gels were spread on a glass slide and stained with 0.002% Rhodamine B solution with ratio water:dye of 1:5 (v/v) (Sigma-Aldrich GmbH, Germany) over 24 h. The samples were analyzed with a CLSM type 510 (Carl Zeiss AG, Germany) using a 543-laser line. Images were taken at a magnification of 20x and analyzed with LAS X software (version 4.5.25531) from Leica Microsystems CMS Gmbh (Germany).

2.5. HMEC

To test the applicability of Cv in PPI meat substitutes, the homogenized Cv biomass was added either in liquid form; C2-H and C2-H-S (soluble fraction), or in powder form; C2-H-D. The extrusion set-up was such that the final concentration of Cv in the extrudate was 10% (w/w) DM. To achieve this, C2-H and C2-H-S were diluted with demineralized water before extrusion. C2-H-D and PPI were mixed for 15 min with a MP50 screw mixer (Prodima Mixers SA, Switzerland) at the maximum speed. 100% PPI was taken as a reference. Meat substitutes were produced using a Clextral Evolum 25 twin-screw extruder (Clextral, Firminy, France) which has a screw diameter of 25 mm and a length/diameter ratio of 40. The barrel temperatures of the 10 sections were set at 30, 50, 70, 90, 100, 120, 120, 125, 125 and 125 °C respectively. The screw speed was set at 240 rpm. A novel and patented rotating cooling die was coupled to the extruder (Beyrer et al., 2020). This rotating die consists of a rotating inner cylinder and a static outer cylinder, which enables well-defined shear in the cooling die (Snel et al., 2022). The rotating speed of this inner cylinder was set at 9 rpm, and the temperature at 85 °C. A twin-screw gravimetric feeder type KCM (K-tron, Niederlenz, Switzerland) was used to feed the dry ingredients into the extruder. Water, or diluted C2-H or C2-H-S, was injected in the second section with a peristaltic pump. Feeding rates were corrected to obtain a final moisture content in the extrudate of 58% and a total throughput of 15 kg/h. Samples were collected in plastic bags, sealed, and immediately frozen in a blast freezer (Electrolux, Sweden).

2.6. Meat substitutes characterization

The extrudates were defrosted overnight at ambient temperature (22 ± 2 °C) before the analysis. Moisture content was measured as a control with a rapid moisture analyzer (HC103 Mettler-Toledo, USA) at the conditions of 150 °C, initial mass of 2.5 g and stop criteria of 1 mg/50 s. The extrudates were cut into 2 mm-thick slices before the measurements. The crude nitrogen content of the meat substitutes was determined by the Kjeldahl method. A conversion factor of 5.5 was used to calculate the protein content. This conversion factor is appropriate for pea protein (Schlangen et al., 2022). The inner texture of the extrudates was exposed by making a small inclination with a sharp knife in the direction of the flow (out of the die) and samples were broken along this cut. Pictures were taken with a digital camera (Nikon DS).

2.6.1. Texture profile analysis (TPA)

TPA was performed using a TA-XT2 texture analyzer (Stable Micro Systems, Surrey, UK) equipped with a 50 kg load cell. The samples were

Table 1
Chemical and thermal properties of intact and HPH-treated Cv suspensions. The different letter means a significant difference $p < 0.05$.

	Chemical properties		Thermal properties			
Samples	Fraction of soluble protein (% w/w)	DM in the soluble fraction (% w/w)	ΔH_1 (J/g DM)	$T_{peak,1}$ (°C)	ΔH_2 (J/g DM)	$T_{peak,2}$ (°C)
C1	17.6 ± 0.2[a]	3.3	1.6 / 1.8	63.9 / 64.1	0.1 / 0.4	90.4 / 94.8
C1-H-90	20.8 ± 0.1[b]	3.6	2.1 / 2.3	63.8 / 64.1	0.1 / 0.4	84.1 / 93.7
C1-H-120	22.8 ± 0.6[b]	4.0	2.3	63.9	0.2 / 0.8	92.1 / 93.5
C1-H-150	25.3 ± 0.6[c]	5.0	2.1 / 2.5	63.6 / 63.7	0.2 / 0.9	91.3 / 91.9

1 and 2 refer to the two main thermal events at 63.7 – 64.0 °C and 88.9 – 92.8 °C, respectively
The initial protein content (f=4.21) of the suspensions was obtained from the SQTS analysis. Fraction of soluble protein values are presented as averages ± SD(n = 3), thermal properties are expressed as individual numbers (n = 2)

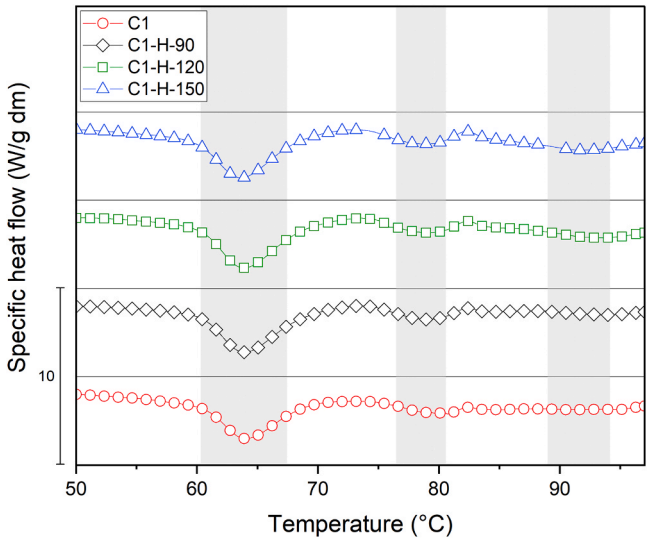

Fig. 3. DSC thermograms of intact and HPH-treated suspensions (n = 2).

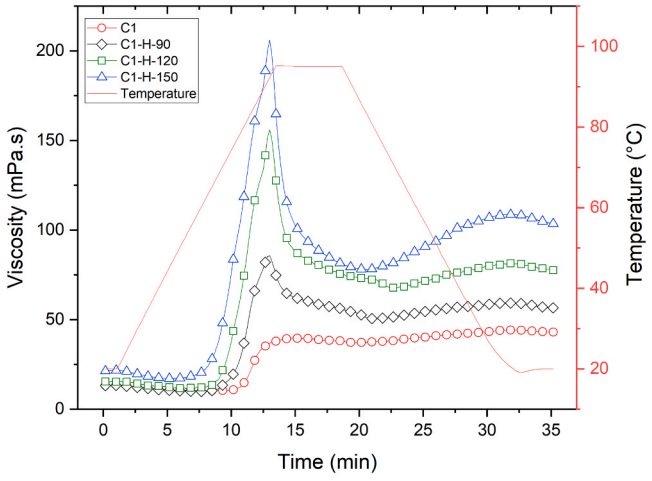

Fig. 4. T-sweep viscosity curves of intact (C1) and HPH-treated suspensions (C1-H-90, C1-H-120, C1-H-150) at 14% DM (n = 3). The full red line indicates the temperature profile.

cut into cylinders of 20 mm in diameter and a height of 1 cm. Subsequently, samples were compressed twice with a 60 mm probe to 30% of the original height with a test speed of 1 mm/second and a waiting time between the two compressions of 5 s. The peak maximum force at first compression was taken as the hardness (Meulleneti, 1998).

Table 3
Crude composition of HPH-treated Cv suspensions in % (w/w) DM and sodium content (mg/kg, wet basis). DM content of the suspensions was of 14%.

Samples	pH (-)	Protein (% w/w) (f=4.21)	Lipid (% w/w)	Carbohydrate (% w/w)	Sodium (mg/kg)
C1-H-150	6.4	36.6	25.8	29.6	110
C2-H	5.4	40.7	16.7	32.0	290

The values were analyzed by an ISO certified, external laboratory (SQTS).

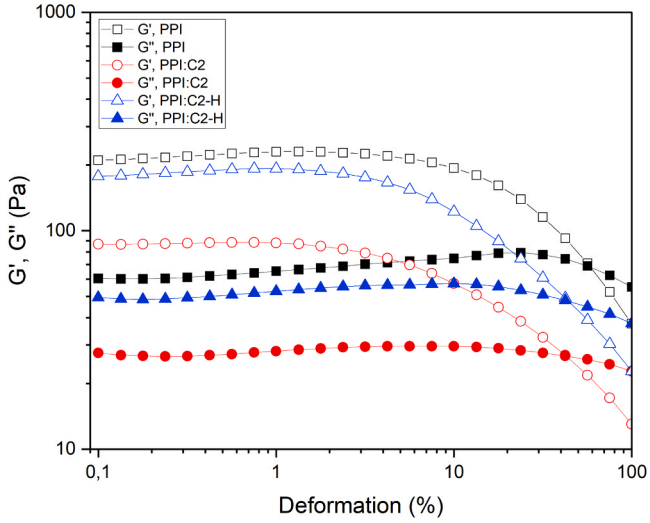

Fig. 5. Storage (G') and loss modulus (G'') of PPI and PPI-Cv gels (17% DM) (n = 3).

2.6.2. Anisotropy index (AI)

The AI was measured to determine the degree of fiber formation of the extrudates. The method is based on the continuous time random walk (CTRW) theory and was developed by Ranasinghesagara et al. (2006). The method has been described by Snel et al. (2022.). Briefly, a red LED (λ = 600 nm) coupled to an optical fiber (diameter = 400 μm) was directed at the 2 x 2 cm sample at a 45° angle. The light reflectance was imaged by a digital camera (Nikon DS) and the AI was calculated based on the deviation from a circular reflection pattern. For an isotropic sample, the AI = 1, meaning the light reflectance was a perfect circle. For an anisotropic sample, the AI > 1.

2.7. Statistical analysis

All the analytical measurements were done in either duplicate (n = 2) or triplicate (n = 3). For duplicates, results were expressed as individual numbers, while triplicates were expressed as average

Table 2
Gelation properties of C1 and C2 before and after processing as measured with a T-sweep. Values are presented as averages ± SD (n = 3). The different letter means a significant difference $p < 0.05$. H: homogenized, S: soluble fraction, D: spray-dried.

Sample	Pressure (MPa)	DM (% w/w)	$\mu_{app,\ initial}$ (mPa s)	$\mu_{app,\ peak}$ (mPa s)	T_{onset} (°C)	T_{peak} (°C)	$\mu_{app,\ final}$ (mPa s)
C1	/	14	13.2 ± 0.3^{a}	36.9 ± 0.9^{a}	76	/	43.0 ± 0.6^{a}
C1-H-90	90	14	13.3 ± 0.2^{a}	85.7 ± 2.7^{b}	67	92.2	56.5 ± 1.1^{ab}
C1-H-120	120	14	15.5 ± 0.6^{b}	156.0 ± 9.3^{c}	67	92.2	77.6 ± 1.7^{ab}
C1-H-150	150	14	21.4 ± 1.4^{c}	206.0 ± 7.6^{d}	62	92.2	103.5 ± 2.5^{b}
C2	/	14	28.0 ± 0.2	36.7 ± 0.8	95.0	/	50.6 ± 0.4
C2-H	150	14	44.6 ± 1.2	404.6 ± 29.9	80.2	91.2	287.0 ± 17.5
C2-H	150	10	21.2 ± 0.8^{a}	145.6 ± 14.3^{a}	59.2	91.2	104.8 ± 5.0^{a}
C2-H-S	150	10	26.0 ± 0.4^{b}	108.7 ± 8.3^{b}	63.2	95.3	89.0 ± 2.2^{a}
C2-H-D	150	10	20.2 ± 0.6^{a}	118.6 ± 1.9^{c}	63.2	95.0	91.7 ± 1.1^{a}

μ_{app} refers to the apparent viscosity, T_{onset} the onset temperature and T_{peak} the temperature at which μ_{app} is maximal.

Table 4
Average storage modulus (G') and loss modulus (G'') at the LVE region. Values are presented as averages ± SD (n = 3). The different letter means a significant difference $p < 0.05$. H: homogenized, S: soluble fraction, D: spray-dried.

Samples	G'_{avg} at LVER (Pa)	G''_{avg} at LVER (Pa)	Relative reduction of G' (%)
PPI	221.7 ± 6.9^{a}	64.9 ± 1.4^{a}	0.0
PPI:C2	86.9 ± 2.0^{b}	27.6 ± 0.5^{b}	60.8
PPI:C2-H	186.1 ± 19.6^{ac}	51.2 ± 3.7^{ac}	16.0
PPI:C2-H-S	140.5 ± 7.8^{c}	41.0 ± 1.9^{c}	36.7
PPI:C2-H-D	$139.0 \pm 18.5.3^{bc}$	39.8 ± 4.9^{bc}	38.5

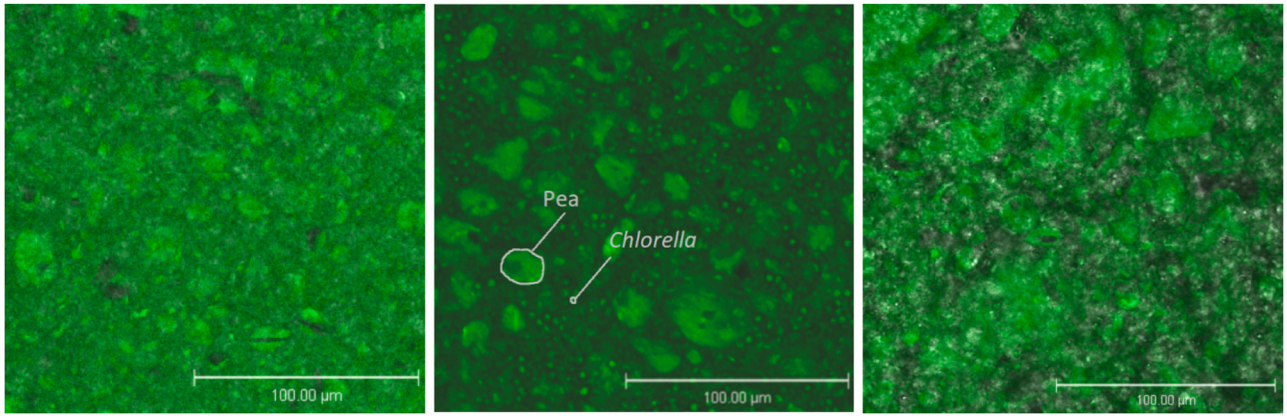

Fig. 6. Gels' microstructure obtained by CLSM imaging. From left to right: PPI, PPI:C2 and PPI:C2-H gels after staining with Rhodamine B solution. Scale = 100 µm.

Table 5
Moisture content (%) and protein content (% wet basis), hardness (N) and anisotropy index of PPI meat substitutes produced with Cv. Different letters indicate different significant groups $p < 0.05$. H: HPH treatment, S: soluble fraction, D: spray-dried.

Sample	Moisture content (%)	Protein content (g/100 g)	Hardness (N)	Anisotropy index (-)
PPI	58.0 ± 0.5^{a}	34.0 / 34.1	113.6 ± 16.0^{a}	1.19 ± 0.02^{a}
PPI:C2-H	57.2 ± 0.1^{b}	30.7 / 31.4	115.5 ± 2.8^{a}	1.13 ± 0.02^{a}
PPI:C2-H-S	57.5 ± 0.2^{ab}	31.5 / 31.9	112.0 ± 2.3^{a}	1.16 ± 0.02^{a}
PPI:C2-H-D	57.1 ± 0.3^{b}	30.1 / 31.5	107.6 ± 1.7^{a}	1.15 ± 0.02^{a}

Moisture content, hardness and anisotropy index were measured in triplicate, and are presented as average ± SD (n = 3), and protein content in duplicate, and expressed as individual values (n = 2)

± standard deviation (SD). Regarding statistical analyses, first normality distribution (Shapiro-Wilk test) and equal variance (Chi-square test for variance) were checked ($p = 0.05$). Statistical significance was estimated by one-way ANOVA, followed by Tukey's post-hoc test. Dunn's test and Welch's ANOVA were used when normality and equal variance were rejected, respectively. When both were rejected, a Kruskal-Wallis test was performed, followed by a Dunn's test for pairwise comparisons. p-values < 0.05 were considered statistically significant. All statistical tests were performed with the software OriginLab® 2022b (OriginLab Corporation, USA).

3. Results and discussion

3.1. Influence of HPH on the microalgae suspension properties

The optimal HPH conditions were identified based on the fraction of soluble protein, gelation capacity, and thermal degradation degree of the 14% DM Cv suspensions. The effect of the operating pressure (90, 120, 150 MPa), the initial product temperature (5, 10, 15, 20, 25 °C), the number of HPH passes (1, 2) as well as the microalgae composition (C1, C2) were considered.

3.1.1. Influence of pressure

First, the HPH-triggered cell disruption was confirmed using microscopic imaging. Consequently, increased extracellular organic matter concentration with increasing pressure was observed in the continuous phase (Fig. 2).

The fraction of soluble protein and the DM in the soluble fraction were measured for validation (Table 1). After HPH at 150 MPa, the respective values increased from 17.6 ± 0.2% (C1, untreated) to 25.3

Fig. 7. Visual appearance of meat substitutes after revealing the inner texture by folding the samples open. From left to right: PPI, PPI:C2-H, PPI:C2-H-D, PPI:C2-H-S.

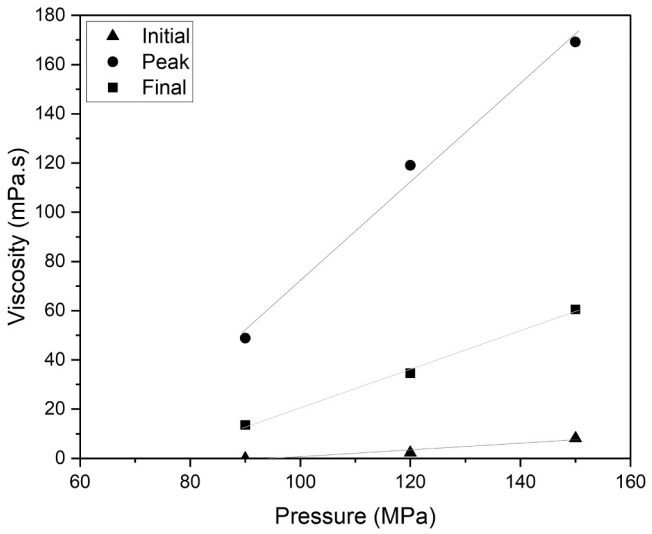

Fig. A1. Linear regression analysis between pressure and initial, peak, and final viscosity. Values were obtained after subtracting μ_{app} of intact cell suspension. The intercept with the x-axis indicates the critical pressure of the cell disruption.

Table A1
Regression analysis parameters.

Viscosity	Initial	Peak	Final
Slope (mPa s/MPa)	0.1	2.0	0.8
Critical pressure (MPa)	94.3	64.0	73.8
R^2	0.94	0.99	1.00

Table A2
Amino acids composition of C1 biomass.

Amino acids	Content (g/100 g powder)	Amino acids	Content (g/100 g powder)
Alanine	1.53	Lysine	1.07
Arginine	9.99	Methionine	0.33
Aspartic acid	3.55	Phenylalanine	0.60
Cystein+Cystine	0.18	Proline	0.61
Glutamic acid	2.95	Serine	0.83
Glycine	0.80	Threonine	0.75
Histidine	0.35	Tryptophan	0.24
Isoleucine	0.51	Tyrosine	0.49
Leucine	1.21	Valine	0.92

Table A3
Initial and calculated (Eq. 4) HPH process temperatures and $\mu_{app,\ peak}$ (at 92.2 °C). Data are presented as individual values (n = 2) .

T_{in} (°C)	T_p (°C)	$\mu_{app,\ peak}$ (mPa s)
5	34	209.0 / 211.5
10	39	146.9 / 150.2
15	54	168.6 / 169.3
20	59	170.8 / 171.5
25	64	119.6 / 120.9

± 0.6% (C1-H-150), and from 3.3% to 5.0%. Spiden et al. (2013) used cell counting to quantitatively measure the cell disruption of *Chlorella sp.* after HPH and found a yield of 50% at 107 MPa. Considering the higher pressure applied (150 MPa), we assumed a yield of cell disruption > 50% and, consequently, we were expecting a higher fraction of soluble protein (> 25.3%). The protein might stick to the cell debris or be organized in granules, explaining the observation.

DSC was performed to evaluate the effect of HPH on the degree of modification of the Cv suspensions after HPH treatment. The reaction enthalpy was similar for untreated and HPH-treated suspensions at different pressures (Table 1, Fig. 3), indicating that the applied HPH at the selected process conditions did not thermally degrade the Cv components. The thermal denaturation temperature of the Cv was detected at 64 °C ($T_{peak,1}$) (Table 1). Waghmare et al. (2016) reported a similar thermal denaturation temperature (60.1 °C) for *Chlorella pyrenoidosa*, mainly attributed to protein denaturation (78.1% (w/w) protein concentration), whereas Ahmed and Kumar (2022) found a temperature of 56.9 °C for Cv, associated with the denaturation of both proteins and carbohydrates. Moreover, other minor endothermic peaks were detected between 78 – 79 °C and 89 – 93 °C (Fig. 3) suggesting that different fractions of biomolecules could be present. Furthermore, a second DSC cycle revealed no peak, confirming that these three thermal events were irreversible (data not shown).

T-sweeps were carried out to determine the heat-induced gelation capacity of the Cv suspensions (Fig. 4). In general, a minimum temperature of 62 °C or T_{onset} was required to induce a viscosity increase, which is also the onset value observed in the DSC. The T_{onset} was higher for the intact cells (76 °C) compared to the HPH-treated cells (62 – 67 °C), indicating a restricted impact on rheological phenomena when intracellular components are inside the cells. Upon heating, the apparent viscosity increased rapidly reaching a peak viscosity ($\mu_{app,peak}$), which was detected at 92.2 °C (Table 2).

Looking at the $\mu_{app,peak}$ of the different treated Cv suspensions (Table 2), these values increased by at least a factor of 2 and up to a factor of 5 with increasing HPH pressure. Additionally, the final viscosity also increased by a factor of 2.5 (Table 2). The intracellular released proteins in combination with cell wall debris and other polysaccharides might swell and hydrate, gaining volume resulting in viscosity increase when reaching a temperature close to 64 °C. At 92 °C, the swollen granules might burst, reducing the viscosity, typically indicating the capacity of these granules to hold water as observed for corn starch (Rincon-Londono et al., 2016). Upon cooling, the viscosity starts to increase again, suggesting cross-linking between the different components, possibly proteins and polysaccharides. Similar viscosity curves were obtained for mixtures of chickpea starch and protein-rich fraction (Sayar et al., 2005). Bernaerts et al. (2017) also compared the viscosity (10.5 s^{-1}, 25 °C) between intact and HPH-treated Cv suspensions (8% DM, pH 6) at 100 MPa, 1 pass, and 4 °C. Although values were not significantly different, the authors measured a viscosity increase of a factor 2 after thermal treatment (121 °C, 5 min). In this study, results confirm that HPH treatment is essential to improve the heat-induced gelation properties of Cv suspensions, as observed with the increase in $\mu_{app,peak}$, triggered by released intracellular components upon cell disruption.

From Table 2, a positive and linear correlation between the operating pressure and $\mu_{app,peak}$ ($R^2 = 0.99$) was obtained (Figure A1, Table A1). Similarly, Magpusao et al. (2021) detected a linear dependency of HPH pressure and cell disruption for *Arthospira platensis, Isochrysis sp.,* and *Tetraselmis sp*. The authors explained their findings by an increase in dynamic viscosity detected in an isothermal measurement (0.1 s^{-1}, 20 °C) after HPH at 30, 60 and 90 MPa. From the linear regression and the intercept with the pressure axis, we estimated a critical pressure of 64 MPa for the HPH treatment to sufficiently disrupt the cells and enhance the heat-induced gelation capacity of 14% DM Cv suspensions.

3.1.2. *Influence of the initial temperature and number of passes*

Besides pressure, the effect of the initial product temperature (Table A3) and a second HPH pass was studied. HPH treatment at 150 MPa and 1 pass was applied on C1 at initial temperatures of 5, 10, 15, 20 and 25 °C. From Eq. 4, an initial temperature equal to or above 25 °C was expected to result in a process temperature of 64 °C or higher, which is sufficient to induce thermal degradation in C1 as seen from the DSC results (Table 1). The highest $\mu_{app,peak}$ value (at 92.2 °C) was

obtained for the HPH-treated suspension at an initial temperature of 5 °C (210 mPa s) (Table A3). Results show a tendency for lower $\mu_{app,peak}$ when higher initial temperatures are used. A gelation capacity reduction of up to 50% at 25 °C initial temperature (120 mPa s) was observed when comparing to 5 °C initial temperature. In conclusion, if thermal-induced effects, such as a first protein denaturation step, are triggered by HPH, the gelation capacity will be reduced due to a lower protein solubility (Rodriguez & Beyrer, 2023). To prevent such reduction after HPH at 150 MPa and 1 pass, an initial temperature of 10 °C or lower is recommended. Finally, a second HPH pass at 150 MPa and 5 °C initial temperature was tested. The fraction of soluble protein and DM in the soluble fraction increased with the second pass and reached 35.8 ± 1.2% and 6.4%, respectively. However, $\mu_{app,peak}$ was not increased with the second pass (from 206.0 to 197.6 mPa s). Thus, the optimal HPH conditions were found to be a pressure of 150 MPa, 1 pass, and 5 – 10 °C initial temperature to achieve sufficient cell disruption while avoiding thermal degradation and consequently optimizing the gelation capacity.

3.1.3. Influence of the composition of different microalgae batches

The biomasses C1 and C2 were available in limited quantities. Pilot scale trials on HMEC were performed with C2, while C1 was used for optimization of DSP, and HPH specifically. For consistency and conclusiveness, some reference values are used to compare C1 and C2. The crude composition of C1-H-150 and C2-H is different, specifically C2-H has a higher protein (+4%) and carbohydrate content (+2%). On the other hand, the lipid content is reduced in C2-H (−9%). This can be explained by differences in the fermentation process and suggests a process control improvement. The initial, peak, and final viscosities of homogenized C2 (C2-H) are twice of those of homogenized C1 (C1-H-150) at the same DM concentration (Table 2). This can be explained by the higher protein and carbohydrate content of C2-H, but also with the lower pH of 5.4, which is close to the isoelectric point of Cv protein (4.5 – 5.5) (Ursu et al., 2014), where the protein net charge and electrostatic repulsion are minimal and protein aggregation is favored. The homogenization effect on the viscosities has the same trend for both batches, C1 and C2, but is more pronounced for C2 (Table 2). This could be once again due to the higher protein and carbohydrate content. Also, the presence of fat reduces the hydrophilicity of the substrate and negatively affects crosslinking of biopolymers upon heating or cooling (Magpusao et al., 2021). C1 contains more fat, and 2.8x lower final viscosity. It is interesting to mention that HPH enhanced the gelation capacity of both Cv suspensions despite their different compositions and pH. This suggests and confirms that HPH is indeed a robust cell wall disruption process, independently of possible batch variations. Beside composition and pH, the pre-handling of the biomass (concentration, freezing and dilution with demineralized water) may influence the disruption and consequently the Cv's gelation properties.

3.2. Influence of further DSP steps on the gelation capacity

In general, DSP of microalgae includes centrifugation for separation of the biomass from the fermentation broth, concentration of the biomass, and drying to obtain microbiologically stable products, as well as sometimes for protein extraction to obtain powdered microalgae protein isolates (Grossmann et al., 2020). Such processing is expected to impact the gelation capacity of microalgae ingredients. Two different DSP steps were performed after HPH, namely centrifugation and spray drying, and their effect on the gelation capacity was studied.

Upon centrifugation, the DM of the suspension reduced from 13.8 ± 0.0% (C2-H) to 10.7 ± 0.1% (C2-H-S), however, the protein content and the nitrogen/carbon ratio were almost not affected (data not shown). In the T-sweep test, the C2-H-S showed significantly lower peak viscosity compared to C2-H at the same DM content (10% (w/w)) (Table 2). This might suggest that the insoluble fraction also contributes to the viscosity increase at heating. The aggregation of intact cells and cell wall material has previously been observed and can be explained by the presence of anionic particles in cell wall polysaccharides, such as sulfate groups and uronic acids (Bernaerts et al., 2017, 2018). Such anionic polymers can gel in the presence of salt, which was detected in the diluted suspension at a level of 220.7 mg sodium/kg (Table 3). To better understand the role of polysaccharides upon heat-induced gelation, a T-sweep was performed after enzymatic hydrolysis. C2-H was incubated with a cellulase complex as well as with an endo-xylanase. The $\mu_{app,\ peak}$ was reduced from 145.6 ± 143 to 103.3 ± 0.7 mPa s, confirming that the peak viscosity is influenced by the presence of polysaccharide molecules.

Next to centrifugation, C2-H was also spray-dried at the pilot scale. The $\mu_{app,peak}$ of the C2-H reduced significantly from 145.6 ± 143 to118.6 ± 1.9 mPa s (Table 2) after spray drying. Drying (T > 100 °C) might denature proteins and thus reduce the solubility during rehydration of the powder (Safi et al., 2013; Soto-Sierra et al., 2018). From these results, we conclude that the improvement of the gelation capacity triggered by the HPH treatment was partially diminished by further DSP. Thus, we anticipate higher gel strength of PPI:Cv blends when using HPH-treated Cv compared to gels made with untreated Cv or HPH-treated Cv submitted to further centrifugation or spray drying steps.

3.3. Influence of Cv addition on the rheological properties of heat-induced PPI gel

Amplitude sweeps were performed to better understand how the incorporation of HPH-treated Cv influenced PPI gel characteristics. Within the LVE region and up to the cross-over point, all preparations showed a G' > G'' (Fig. 5) indicating a viscoelastic gel or solid behavior (Mezger, 2014). The yield point at the end of the LVE region was detected at a strain 2.4–2.8% for the PPI-Cv gels, and 5.6% for the PPI gel (data not shown) suggesting a more brittle structure for PPI-Cv gels. Similarly, the G' plateau value at the LVE region was significantly reduced (60.8%) compared to PPI gel when substituting PPI with untreated biomass (PPI:C2) (Table 4). This G' reduction was not significant when HPH-treated biomass (PPI:C2-H) was used instead. The effect of HPH treatment on G' of microalgae has been shown previously (Ahmed & Kumar, 2022; Bernaerts et al., 2018; Nunes et al., 2020). Nunes et al. (2020) did a similar experiment where untreated Cv and HPH-treated Cv (at 340 MPa) were added to wheat dough observing that the overall G' decreased upon 1% (w/w) Cv addition, however, this decrease was less significant when using HPH-treated Cv. Similarly, Ahmed and Kumar (2022) observed an increase in G' of more than 1 log when Cv was treated with HPH, and Bernaerts et al. (2017) a 4x G' increase after HPH and thermal treatment of Cv. They attributed these findings to the effective cell disruption from the HPH treatment and the subsequent release of intracellular material, and protein aggregation after thermal treatment. These results correspond as well to the observations in viscosity increase (Section 3.1) after heat-induced gelation of the HPH-treated Cv.

Removing the insoluble fraction in the centrifugation step (PPI:C2-H-S), resulted in a significant reduction (37%) of G'. However, the major gelling effect was provided by the soluble fraction. Also, spray-drying the whole homogenized biomass (PPI:C2-H-D) reduced the gelling ability by 38% compared to the non-homogenized, non-dried biomass. This could be possibly due to additional protein denaturation effects (Table 4). These values are in between the addition of fresh (C2, 60.8%) and wet HPH-treated biomass (C2-H, 16.0%) and correlate well with our previous observations that HPH alone was more prone to enhance gelation compared to further centrifugation or spray drying steps (Section 3.2). However, for all forms of Cv, the yield strain was reduced in a similar magnitude indicating that adding 10% (w/w) of Cv to PPI results in a more brittle gel, independent of the Cv treatment or DSP.

CLSM was done on PPI, PPI:C2 and PPI:C2-H gels to analyze their microstructure (Fig. 6). The significant reduction of gel strength as a

result of the addition of untreated Cv (C2) (60.8%) can be explained by a transition from a mono- toward a bi-phasic gel. Indeed, in the PPI:C2 gel, pea protein aggregates (30 – 50 μm) were separated by a phase containing intact Cv cells (2 – 10 μm). In contrast, the microstructure of PPI:C2-H gel showed a more homogenous phase, like PPI gel, and therefore the least G' relative reduction (16.0%).

3.4. HMEC application

PPI and PPI-Cv meat substitutes were produced by HMEC and compared in terms of color, texture, and anisotropy. The addition of 10% (w/w) HPH-treated Cv, either in liquid or spray-dried forms, did not lead to instabilities during HMEC. The final moisture and protein content of the extrudates were reduced upon Cv addition (Table 5). This decrease was significant for extrudates PPI:C2-H and PPI:C2-H-D. The lower protein content in the PPI-Cv extrudates could be expected since the protein content of Cv (40.7% (w/w)) was approximately 2x lower than in PPI. Visual observations showed no clear difference between the samples, although the PPI extrudate looked more fibrous and PPI:C2-H-D seemed slightly more yellow (Fig. 7).

Despite the clear differences in G' observed previously after 10% (w/w) Cv incorporation in PPI gels (Section 3.3), no significant effect on hardness or anisotropy index was observed in the extrudates (Table 5). This is probably due to the much higher DM content of the extrudates, resulting in a more jammed gel, instead of the soft gel obtained at 17% DM as tested with rheology. In this jammed gel, Cv probably acts as a filler. This has been shown before for undisrupted microalgae and pea protein gels (Batista et al., 2011). Palanisamy et al. (2019) observed a similar effect for the addition of 15% dried *Arthospira platensis* to lupin meat substitutes, for which no significant difference in cutting strength was measured. Apart from hardness, cohesiveness, springiness, and chewiness of the samples were also not significantly different (data not shown). Furthermore, the anisotropy indexes were all above 1 and not significantly different (Table 5), indicating that the anisotropic meat substitutes showed similar level of fibrousness.

4. Conclusions and perspectives

HPH-treated biomass from yellow Cv was studied as an ingredient for meat substitutes produced by HMEC. Optimal conditions for HPH were found at an operating pressure of 150 MPa and an initial product temperature below 10 °C. The heat-induced gelation capacity of both untreated and HPH-treated Cv suspensions was monitored by T-sweep measurements. We observed an up to 10x increase in peak viscosity for HPH-treated, compared to the untreated Cv biomass. It is suggested that both, soluble (released intracellular materials such as proteins) and insoluble fractions, contribute to the viscosity development upon heating. The positive impact of cell disruption by HPH on controlling PPI-Cv gels' structure was confirmed by strain sweeps and CLSM. Additional removal of insoluble matter from the Cv biomass or drying steps after HPH treatment did not lead to improved properties. The addition of 10% (w/w) HPH-treated Cv, wet or dry, to pea meat substitutes did not lead to significant differences in hardness, visual appearance or anisotropy index. HPH-treated Cv biomass is an interesting ingredient to consider when designing sustainable and nutritious plant-based meat substitutes.

Funding

This project was financially supported by the Swiss Innovation Agency "Innosuisse" under application number 36440.1 IP-LS and the Canton of Fribourg (Switzerland) in the frame of the flagship program "biomass valorization" 2022.

Declaration of Competing Interest

The authors declare that they have no known competing financial interests or personal relationships that could have appeared to influence the work reported in this paper.

Acknowledgments

The authors thank Frédéric Maruel and Julien Pott (University of Applied Sciences and Arts Western Switzerland, School of Engineering) for their help and assistance during Pilot Plant trials and analyses. Thanks are also addressed to Jarno Gieteling and Dr. Norbert de Ruijter from the Wageningen Light Microscopy Center (WLMC) for their help in CLSM sample preparation and imaging. Finally, thanks to Ailsa Moodycliffe (University of Applied Sciences and Arts Western Switzerland, School of Engineering) for proofreading the manuscript.

Appendices

Fig. A1 and Table A1, Table A2 and Table A3.

References

Ahmed, J., & Kumar, V. (2022). Effect of high-pressure treatment on oscillatory rheology, particle size distribution and microstructure of microalgae *Chlorella vulgaris* and *Arthospira platensis*. *Algal Research, 62*. https://doi.org/10.1016/j.algal.2021.102617

Barka, A., & Blecker, C. (2016). Microalgae as a potential source of single-cell proteins. A review. *Biotechnol Agron Soc Environ* (Vol. 20)(Issue 3).

Batista, A. P., Nunes, M. C., Raymundo, A., Gouveia, L., Sousa, I., Cordobés, F., Guerrero, A., & Franco, J. M. (2011). Microalgae biomass interaction in biopolymer gelled systems. *Food Hydrocolloids, 25*(4), 817–825. https://doi.org/10.1016/j.foodhyd.2010.09.018

Becker, E. W. (2007). Micro-algae as a source of protein. *Biotechnology Advances* (Vol. 25, (Issue 2), 207–210. https://doi.org/10.1016/j.biotechadv.2006.11.002

Bernaerts, T. M. M., Panozzo, A., Doumen, V., Foubert, I., Gheysen, L., Goiris, K., Moldenaers, P., Hendrickx, M. E., & van Loey, A. M. (2017). Microalgal biomass as a (multi)functional ingredient in food products: Rheological properties of microalgal suspensions as affected by mechanical and thermal processing. *Algal Research, 25*, 452–463. https://doi.org/10.1016/j.algal.2017.05.014

Bernaerts, T. M. M., Panozzo, A., Verhaegen, K. A. F., Gheysen, L., Foubert, I., Moldenaers, P., Hendrickx, M. E., & van Loey, A. M. (2018). Impact of different sequences of mechanical and thermal processing on the rheological properties of *Porphyridium cruentum* and *Chlorella vulgaris* as functional food ingredients. *Food and Function, 9*(4), 2433–2446. https://doi.org/10.1039/c8fo00261d

Beyrer, M., Cachelin, C., & Rapillard L. (2020). *Nozzle for extruding a material rich in protein and water, as well as an extrusion machine comprising such a nozzle. Patent n° WO2022018084A1.*

Bito, T., Okumura, E., Fujishima, M., & Watanabe, F. (2020). Potential of *Chlorella* as a dietary supplement to promote human health (MDPI AG) *Nutrients* (Vol. 12,(Issue 9), 1–21. https://doi.org/10.3390/nu12092524.

Canelli, G., Neutsch, L., Carpine, R., Tevere, S., Giuffrida, F., Rohfritsch, Z., Dionisi, F., Bolten, C. J., & Mathys, A. (2020a). *Chlorella vulgaris* in a heterotrophic bioprocess: Study of the lipid bioaccessibility and oxidative stability. *Algal Research*, 45. https://doi.org/10.1016/j.algal.2019.101754

Canelli, G., Tarnutzer, C., Carpine, R., Neutsch, L., Bolten, C. J., Dionisi, F., & Mathys, A. (2020b). Biochemical and nutritional evaluation of *Chlorella* and *Auxenochlorella* biomasses relevant for food application. *Frontiers in Nutrition, 7*, 1–9. https://doi.org/10.3389/fnut.2020.565996

Caporgno, M. P., & Mathys, A. (2018). Trends in microalgae incorporation into innovative food products with potential health benefits. In *In Frontiers in Nutrition* (Vol. 5). Frontiers Media S.A.,. https://doi.org/10.3389/fnut.2018.00058

Caporgno, M. P., Haberkorn, I., Böcker, L., & Mathys, A. (2019). Cultivation of *Chlorella protothecoides* under different growth modes and its utilization in oil/water emulsions. *Bioresource Technology, 288*(May), Article 121476. https://doi.org/10.1016/j.biortech.2019.121476

Carullo, D., Abera, B. D., Casazza, A. A., Donsì, F., Perego, P., Ferrari, G., & Pataro, G. (2018). Effect of pulsed electric fields and high-pressure homogenization on the aqueous extraction of intracellular compounds from the microalgae *Chlorella vulgaris*. *Algal Research, 31*, 60–69. https://doi.org/10.1016/j.algal.2018.01.017

Chen, C., Chaudhary, A., & Mathys, A. (2019). Dietary change scenarios and implications for environmental, nutrition, human health and economic dimensions of food sustainability. *Nutrients, 11*(4), 1–21. https://doi.org/10.3390/nu11040856

Cornet, S. H. V., Snel, S. J. E., Schreuders, F. K. G., van der Sman, R. G. M., Beyrer, M., & van der Goot, A. J. (2022). Thermo-mechanical processing of plant proteins using shear cell and high-moisture extrusion cooking. In *Critical Reviews in Food Science and Nutrition* (Vol. 62, pp. 3264–3280). Taylor and Francis Ltd,. https://doi.org/10.1080/10408398.2020.1864618

Dekkers, B. L., Boom, R. M., & van der Goot, A. J. (2018). Structuring processes for meat analogues. *Trends in Food Science and Technology, 81*, 25–36. https://doi.org/10.1016/j.tifs.2018.08.011

Demarco, M., de Moraes, Oliveira, Matos, J., Derner, Â. P., de Farias Neves, R. B., & F., & Tribuzi, G. (2022). Digestibility, bioaccessibility and bioactivity of compounds from

algae. In *In Trends in Food Science and Technology* (Vol. 121, pp. 114–128). Elsevier Ltd,. https://doi.org/10.1016/j.tifs.2022.02.004

Fu, Y., Chen, T., Chen, S. H. Y., Liu, B., Sun, P., Sun, H., & Chen, F. (2021). The potentials and challenges of using microalgae as an ingredient to produce meat analogues. *Trends in Food Science and Technology, 112*(September 2020), 188–200. https://doi.org/10.1016/j.tifs.2021.03.050

Grahl, S., Palanisamy, M., Strack, M., Meier-Dinkel, L., Toepfl, S., & Mörlein, D. (2018). Towards more sustainable meat alternatives: How technical parameters affect the sensory properties of extrusion products derived from soy and algae. *Journal of Cleaner Production, 198*, 962–971. https://doi.org/10.1016/j.jclepro.2018.07.041

Grossmann, L., Hinrichs, J., & Weiss, J. (2020). Cultivation and downstream processing of microalgae and cyanobacteria to generate protein-based technofunctional food ingredients. *Critical Reviews in Food Science and Nutrition, 60*(17), 2961–2989. https://doi.org/10.1080/10408398.2019.1672137

Imamoglu, E. (2015). Simulation design for microalgal protein optimization. *Bioengineered, 6*(6), 342–346. https://doi.org/10.1080/21655979.2015.1098792

Kusmayadi, A., Leong, Y. K., Yen, H. W., Huang, C. Y., & Chang, J. S. (2021). Microalgae as sustainable food and feed sources for animals and humans – Biotechnological and environmental aspects. *Chemosphere*, 271. https://doi.org/10.1016/j.chemosphere.2021.129800

Lafarga, T. (2019). Effect of microalgal biomass incorporation into foods: Nutritional and sensorial attributes of the end products. In *In Algal Research* (Vol. 41). Elsevier B.V,. https://doi.org/10.1016/j.algal.2019.101566

Magpusao, J., Giteru, S., Oey, I., & Kebede, B. (2021). Effect of high-pressure homogenization on microstructural and rheological properties of *A. platensis, Isochrysis, Nannochloropsis* and *Tetraselmis species*. *Algal Research*, *56*. https://doi.org/10.1016/j.algal.2021.102327

Meulleneti, J. (1998). Relationship between sensory and instrumental texture profile attributes. *Journal of Sensory Studies, 13*(1998), 77–93.

Mezger, T.G. (2014). *The Rheology Handbook:* 4th Edition. Vincentz Network.

Nunes, M. C., Graça, C., Vlaisavljević, S., Tenreiro, A., Sousa, I., & Raymundo, A. (2020). Microalgal cell disruption: Effect on the bioactivity and rheology of wheat bread. *Algal Research*, *45*. https://doi.org/10.1016/j.algal.2019.101749

Oppen, D., Grossmann, L., & Weiss, J. (2022). Insights into characterizing and producing anisotropic food structures. *Critical Reviews in Food Science and Nutrition, 0*(0), 1–19. https://doi.org/10.1080/10408398.2022.2113365

Osorio-Arias, J. C., Vega-Castro, O., & Martinez-Monteagudo, S. I. (2020). Fundamentals of high-pressure homogenization of foods. *Innovative Food Processing Technologies: A Comprehensive Review* (pp. 244–273). Elsevier,. https://doi.org/10.1016/b978-0-08-100596-5.23021-7

Palanisamy, M., Töpfl, S., Berger, R. G., & Hertel, C. (2019). Physico-chemical and nutritional properties of meat analogues based on Spirulina/lupin protein mixtures. *European Food Research and Technology, 245*(9), 1889–1898. https://doi.org/10.1007/s00217-019-03298-w

Ranasinghesagara, J., Hsieh, F., & Yao, G. (2006). A photon migration method for characterizing fiber formation in meat analogs. *Journal of Food Science, 71*(5). https://doi.org/10.1111/j.1750-3841.2006.00038.x

Rincon-Londono, N., Vega-Rojas, L. J., Contreras-Padilla, M., Acosta-Osorio, A. A., & Rodríguez-García, M. E. (2016). Analysis of the pasting profile in corn starch: Structural, morphological, and thermal transformations, Part I. *International Journal of Biological Macromolecules, 91*, 106–114.

Safi, C., Charton, M., Pignolet, O., Silvestre, F., Vaca-Garcia, C., & Pontalier, P. Y. (2013). Influence of microalgae cell wall characteristics on protein extractability and determination of nitrogen-to-protein conversion factors. *Journal of Applied Phycology, 25*(2), 523–529. https://doi.org/10.1007/s10811-012-9886-1

Safi, C., Zebib, B., Merah, O., Pontalier, P. Y., & Vaca-Garcia, C. (2014). Morphology, composition, production, processing and applications of *Chlorella vulgaris*: A review. *Renewable and Sustainable Energy Reviews, 35*, 265–278. https://doi.org/10.1016/j.rser.2014.04.007

Safi, C., Olivieri, G., Campos, R. P., Engelen-Smit, N., Mulder, W. J., van den Broek, L. A. M., & Sijtsma, L. (2017). Biorefinery of microalgal soluble proteins by sequential processing and membrane filtration. *Bioresource Technology, 225*, 151–158. https://doi.org/10.1016/j.biortech.2016.11.068

Sayar, S., Koksel, H., & Turhan, M. (2005). The effects of protein-rich fraction and defatting on pasting behavior of chickpea starch. *Starch/Starke, 57*(12), 599–604. https://doi.org/10.1002/star.200500397

Schlangen, M., Taghian Dinani, S., Schutyser, M. A. I., & van der Goot, A. J. (2022). Dry fractionation to produce functional fractions from mung bean, yellow pea and cowpea flour. *Innovative Food Science and Emerging Technologies, 78*, Article 103018. https://doi.org/10.1016/j.ifset.2022.103018

Seyfabadi, J., Ramezanpour, Z., & Khoeyi, Z. A. (2011). Protein, fatty acid, and pigment content of *Chlorella vulgaris* under different light regimes. *Journal of Applied Phycology, 23*(4), 721–726. https://doi.org/10.1007/s10811-010-9569-8

Show, K. Y., Lee, D. J., Tay, J. H., Lee, T. M., & Chang, J. S. (2015). Microalgal drying and cell disruption - Recent advances. In *Bioresource Technology* (Vol. 184, pp. 258–266). Elsevier Ltd,. https://doi.org/10.1016/j.biortech.2014.10.139

Smetana, S., Sandmann, M., Rohn, S., Pleissner, D., & Heinz, V. (2017). Autotrophic and heterotrophic microalgae and cyanobacteria cultivation for food and feed: life cycle assessment. *Bioresource Technology, 245*, 162–170. https://doi.org/10.1016/j.biortech.2017.08.113

Snel, S. J. E., Bellwald, Y., van der Goot, A. J., & Beyrer, M. (2022). Novel rotating die coupled to a twin-screw extruder as a new route to produce meat analogues with soy, pea and gluten. *Innovative Food Science & Emerging Technologies, 81*, Article 103152. https://doi.org/10.1016/j.ifset.2022.103152

Soto-Sierra, L., Stoykova, P., & Nikolov, Z. L. (2018). Extraction and fractionation of microalgae-based protein products. In *In Algal Research* (Vol. 36, pp. 175–192). Elsevier B.V,. https://doi.org/10.1016/j.algal.2018.10.023

Spiden, E. M., Yap, B. H. J., Hill, D. R. A., Kentish, S. E., Scales, P. J., & Martin, G. J. O. (2013). Quantitative evaluation of the ease of rupture of industrially promising microalgae by high pressure homogenization. *Bioresource Technology, 140*, 165–171. https://doi.org/10.1016/j.biortech.2013.04.074

Tanger, C., Engel, J., & Kulozik, U. (2020). Influence of extraction conditions on the conformational alteration of pea protein extracted from pea flour. *Food Hydrocolloids*, *107*. https://doi.org/10.1016/j.foodhyd.2020.105949

Uran, M., Caporgno, M., Zinn, M., Tremblay, P., & Pott, J. (2021). Methods of growing microalgae & products thereof. *Patent n°EP4122330A1*. ⟨https://www.epo.org/⟩.

Ursu, A. V., Marcati, A., Sayd, T., Sante-Lhoutellier, V., Djelveh, G., & Michaud, P. (2014). Extraction, fractionation and functional properties of proteins from the microalgae *Chlorella vulgaris*. *Bioresource Technology, 157*, 134–139. https://doi.org/10.1016/j.biortech.2014.01.071

Waghmare, A. G., Salve, M. K., LeBlanc, J. G., & Arya, S. S. (2016). Concentration and characterization of microalgae proteins from *Chlorella pyrenoidosa*. *Bioresources and Bioprocessing, 3*(1). https://doi.org/10.1186/s40643-016-0094-8

Wang, Y., Tibbetts, S. M., Berrue, F., McGinn, P. J., MacQuarrie, S. P., Puttaswamy, A., Patelakis, S., Schmidt, D., Melanson, R., & MacKenzie, S. E. (2020). A rat study to evaluate the protein quality of three green microalgal species and the impact of mechanical cell wall disruption. *Foods, 9*(11). https://doi.org/10.3390/foods9111531

Yao, G., Liu, K. S., & Hsieh, F. (2004). A new method for characterizing fiber formation in meat analogs during high-moisture extrusion. *Journal of Food Science, 69*(7), 303–307. https://doi.org/10.1111/j.1365-2621.2004.tb13634.x